JCTC Journal of Chemical Theory and Computation

Theoretical Study of Intramolecular, CH−X (X = N, O, Cl), Hydrogen Bonds in Thiazole Derivatives†

Miguel Castro,*,‡ Inés Nicolás-Vázquez,‡,§ Jesús I. Zavala,‡ F. Sánchez-Viesca,|| and Martha Berros||

Departamento de Física y Química Teórica and Departamento de Química Orgánica, DEPg., Facultad de Química, Universidad Nacional Autónoma de México, México D.F., C.P. 04510, México, and Departamento de Ciencias Químicas, Facultad de Estudios Superiores Cuautitlán, Campo 1, Universidad Nacional Autónoma de México, Cuautitlán Izcalli, C. P. 54740, Edo. de México, México

Received November 14, 2006

Abstract: CH−X (X = N, O, or Cl) hydrogen bonds formed intramolecularly in 2-methyl-4-(2-chloro-4,5-dimethoxyphenyl)thiazole (**Ia)**, 2-amino-4-(2-chloro-4,5-dimethoxy phenyl)thiazole (**Ib**), 2-amino-4-(2,4,5-trimethoxyphenyl)thiazole (**Ic**), and 2-methyl-4-(2,4,5-trimethoxyphenyl)thiazole (**Id**) were studied by means of all-electron calculations performed with the B3LYP/6-311++G-(d,p) method. Computed ground states, in the gas phase, show the presence of a single H-bond, CH−Cl, in each **Ia** and **Ib** moiety, and two H-bonds, CH−N and CH−O, for each **Ic** and **Id** molecule. H−Cl, H−N, and H−O distances are shorter than the sum of the X and H van der Waals radii. H-bond energies of ≅2.0 kcal/mol were estimated for **Ia** and **Ib** and ≅4.0 kcal/mol for **Ic** and **Id.** These results agree with those of the theory of atoms in molecules, since bond critical points were found for these H−X bonds. Finally, the chemical shifts in the ^{1}H NMR were calculated by the GIAO method; in **Ia** and **Ib** they are merely due to the different topological positions of the H atoms. But in **Ic** and **Id** the shifts of H−N and H−O have signatures of H-bond formations.

I. Introduction

Thiazoles,[1] with aryl groups as substituents, may trigger the formation of intramolecular hydrogen bonding, that is favored both by the free rotation around the C−C bond, joining the thiazole and phenyl rings and by the kind of heteroatoms or functional groups attached to the rings. The physicochemical properties of these thiazole derivatives may depend on the type of H-bonds that these compounds can form. In fact, the use of ^{1}H NMR and X-ray diffraction methods[2,3] with this sort of species has suggested the formation of weak intramolecular H-bonds involving aromatic hydrogens. Even more, the results indicate the existence of different rotamers due to the intramolecular H-bonds,[2,3] suggesting that some aromatic hydrogens in benzene rings show paramagnetic shifts in their ^{1}H NMR spectra, as an effect of the possible formation of H-bonds. In general, hydrogen bonding became of great interest in the last few decades due to its importance in different biochemical processes.[4,5] In particular, intramolecular H-bonds are important because they can produce changes in the molecular conformation, affecting consequently the properties of thiazole derivatives.[6]

Conventional H-bonds are usually defined as a Y−H−X interaction, where Y−H is the typical covalent bond being the proton donating moiety and X the accepting center.[7−11] The formation and binding energy of a conventional H-bond depends on the Lewis acidity of the Y−H bond and on the

† Dedicated to Professor Dennis R. Salahub on the occasion of his 60th birthday.

* Corresponding author e-mail: castro@quetzal.pquim.unam.mx.
‡ Departamento de Física y Química Teórica, Universidad Nacional Autónoma de México.
§ Departamento de Química Orgánica, Universidad Nacional Autónoma de México.
|| Departamento de Ciencias Químicas, Universidad Nacional Autónoma de México.

10.1021/ct600336r CCC: $37.00
Published on Web 04/12/2007

Lewis basicity of the X moiety; such an acidity-basicity requirement is fulfilled when Y and X are moderate or highly electronegative atoms such as oxygen or fluorine.[7] More recently, new types of hydrogen bonds have been characterized,[7−9] and they were recorded as nonconventional hydrogen bonds. One way to achieve the formation of a nonconventional H-bond is when the C−H bond acts as donor. Nonconventional CH−X hydrogen bonds will be addressed in the present research; that is, when the C−H bonds, either from the thiazole or phenyl rings, behave as the Lewis acid, whereas the X proton acceptors are the N atom of the thiazole ring and/or the Cl and O atoms, attached to the phenyl group. Therefore, the objective of this work is to characterize, by means of theoretical calculations, the formation of nonconventional intramolecular H-bonds in the polysubstituted arylthiazole derivatives. We will also show how these results may account for the particular crystal packing of these species. This is accomplished in terms of the calculated geometrical and energetic properties and on the Bader theory[12] of atoms in molecules for a study of electronic densities and Laplacians at bond critical points of the CH−X (X = N, Cl, and O) bonds. The topology of ρ and $\nabla^2\rho$ has proved useful to depict complex H-bonds.[13] In this work, aside from these parameters the determination of chemical shifts was also addressed. For these purposes, the Density Functional Theory (DFT) methodology was used.[14]

II. Computational Methodology

Full optimization, which includes relaxation of geometry and electronic structure of four polysubstituted arylthiazoles derivatives, 2-methyl-4-(2-chloro-4,5-dimethoxyphenyl)thiazole (**Ia**), 2-amino-4-(2-chloro-4,5-dimethoxyphenyl)thiazole (**Ib**), 2-amino-4-(2,4,5-trimethoxyphenyl)thiazole (**Ic**), and 2-methyl-4-(2,4,5-trimethoxyphenyl)thiazole (**Id**), was carried out with the B3LYP/6-311++G(d,p) method.[15,16] The B3LYP functional has been widely used for the study of weak hydrogen bonds.[17−24] All-electron calculations were performed with the aid of the Gaussian 98 program.[25] In this way the GS (ground-state) geometries of **Ia**−**Id** were computed. Geometric, energetic, topological, and spectroscopic (chemical shifts) parameters were used for the characterization of these H-bonds. For each compound was computed, using Gaussian-98, the GS wave function, which was further applied for the "atoms in molecules" (AIM) analysis[12] to find bond critical points (BCPs) and associated ring critical points (RCPs). AIM calculations were performed with the aid of the AIM2000 program.[26] The BCPs and RCPs were analyzed in terms of electron densities, ρ, and their Laplacians, $\nabla^2\rho$. AIM2000 gives Laplacians that need to be multiplied by −4 to obtain the correct values;[27] our reported values are corrected. A vibrational analysis for all species studied in this work was made, finding that the optimized geometries correspond to a minimum on the potential energy surface (PES), since all the computed frequencies were real. The chemical shifts were calculated for these GS structures by means of the gauge invariant atomic orbital (GIAO) method.[28,29]

III. Results and Discussion

IIIa. Geometrical and Energetic Results. The B3LYP/6-311++G(d,p) GS geometries for the bare **Ia**−**Id** derivatives are shown in Figure 1. The structures of **Ia** and **Ib** were determined by means of X-ray diffraction;[3] they are indicated in Figure 2. Some selected equilibrium bond lengths and bond and dihedral angles are reported in Tables 1−3 of the Supporting Information, where they are compared against their experimental counterparts. The theoretical results show a reasonable agreement with the experiment. For **Ia,** X-rays yields a quasi planar structure with a dihedral $C_7-C_6-C_4-C_5$ angle of 6.54° and $Cl-H_{13}$ and N_3-H_{12} contacts of 2.476 and 2.361 Å, respectively. While the theory indicates a less planar geometry, since a bigger value, 25.1°, was obtained for that angle. The calculated $Cl-H_{13}$ distance, 2.640 Å, differs from the X-ray assignment, while the theoretical result for N_3-H_{12}, 2.385 Å, is close to the X-ray determination. Crystal packing effects account partially for these structural differences. Similarly, X-ray results assign for **Ib** a nonplanar geometry with a $C_7-C_6-C_4-C_5$ angle of 52.27°, while DFT calculations yield a smaller, 25.30°, angle. These differences are also mainly due from crystal packing effects. Indeed, as shown in Figure 2, in the solid phase, each **Ib** unit is strongly bonded to other **Ib** moieties, accounting for the differences of the structural parameters of **Ib** in the gas phase and **Ib** in the crystal. Moreover, the experimentally determined[3] $Cl-H_{13}$ and N_3-H_{12} distances for **Ib** (2.954 and 2.780 Å, respectively) are significantly longer than the theoretical values, 2.640 and 2.378 Å, and they are also longer than the corresponding experimental values for **Ia.** These features are also a consequence of the more open geometry observed for **Ib**; see the **Ib-Exp** structure in Figure 2.

Another source of discrepancy is the C−H distance, and as determined by X-ray crystallography it is about 0.1 Å shorter than the actual distance to the proton that would be determined by neutron diffraction.[30] Correcting, the C−H bond lengths of **Ia** and **Ib**, 1.03 Å, are nearer to the theoretical results, 1.07−1.08 Å. However, for **Ia-Exp**, the corrected Cl−H (2.42 Å) and N−H (2.34 Å) distances still differ noticeably from the theoretical results for bare **Ia**. Whereas the C−H corrections for **Ib-Exp** yield negligible changes for the O−H (2.938 Å) and N−H (2.775 Å) lengths. Overall, neutron diffraction corrections yield small changes for the CH−X (X = N, Cl, and O) distances, which is due to the nonlinearity of these contacts. As will be shown below, CH−X distances and CH−X linearity, or nonlinearity, are very important for determining the formation, or absence, of an intramolecular H-bond. On the other hand, in the literature are reported values of 6.2° up to 58.8° for the $C_7-C_6-C_4-C_5$ angles of 2,4-disubstituted thiazoles;[3] the present results fall in this range.

Moving now to **Ic** and **Id**, they have the same value, 2.240 Å, for the $O_{14}-H_{13}$ distance and similar N_3-H_{12} separations of 2.340−2.350 Å. Moreover, these compounds are planar since the dihedral $C_5-C_4-C_6-C_7$ angles are close to zero (0.01−1.06°); see the structures **Ic** and **Id** in Figure 1. For **Ic** and **Id** there are no experimental geometries reported. Overall, the **Ia**−**Id** structures suggest the formation of weak

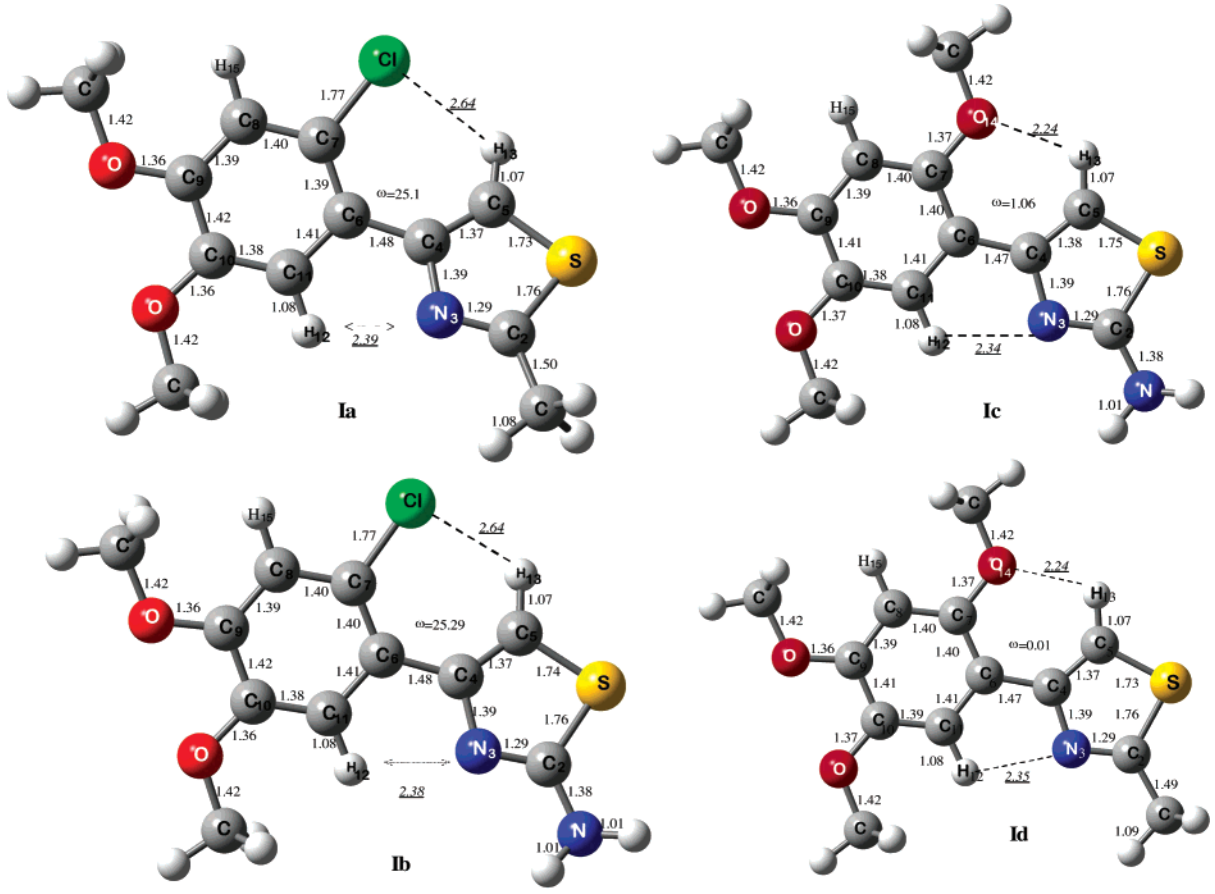

Figure 1. Optimized B3LYP/6-311++G(d,p) geometries for the bare **Ia**−**Id** derivatives. The CH—Cl, CH—N, and CH—O distances, in Å, are indicated as well as the dihedral angles, $\omega = C_7C_6C_4C_5$, in deg.

intramolecular H-bonds. Thus, we will continue with the analysis of this type of bonds.

A geometrical criteria for the formation of a CH—X hydrogen bond is that the distance between the proton and the acceptor atoms (H—X) should be shorter than the sum of their van der Waals radii.[10] The theoretical results show $C_{11}H_{12}$—N_3 contacts of 2.378−2.385 Å for **Ia** and **Ib.** Slightly shorter, 2.341−2.349 Å, contacts were obtained for **Ic** and **Id**. In both cases, these CH—N contacts are meaningfully smaller than the sum of the van der Waals radii[31] of the N (1.5 Å) and H (1.1 Å) atoms, suggesting the intramolecular $C_{11}H_{12}$—N_3 H-bond formation for each **Ia**−**Id** derivative. In fact, these contacts are even shorter than the reported values, 2.52−2.72 Å, for this kind of CH—N bond.[32] Moreover, the calculated C_{11}—N_3 distances, 2.804 and 2.799 Å, in the $C_{11}H_{12}$—N_3 contacts of **Ia** and **Ib** are relatively close to the X-ray values,[3] 2.749 and 2.990 Å; which are smaller than the C—N distance, 3.41 Å, reported for a CH—N H-bond.[30] Similarly, the C_{11}—N_3 distances for **Ic,** 2.786 Å, and **Id**, 2.792 Å, are also smaller than the reported value.[30] However, it has been shown that this sort of geometrical criteria, particularly for weak H-bonds, is doubtful.[7] In fact, as shown below the energetic and topological criteria deny the formation of intramolecular $C_{11}H_{12}$—N_3 bonds in **Ia** and **Ib.** The calculated nonplanar structures of **Ia** and **Ib** are reflected in the absence of these H—N bonds.

On the other hand, the calculated C_5H_{13}—Cl contacts for **Ia** and **Ib,** 2.64 Å, are noticeably smaller than the sum of the van der Waals radii of the Cl (1.7 Å) and H (1.1 Å) atoms; they are also in agreement with the experimental values, 2.57−2.94 Å, reported for this type of H-bond.[30] More recently, Moro et al.[33] described the formation of intramolecular C−H—Cl bonding. In their studied compounds, the H—Cl distances are 2.69 and 2.76 Å; our computed value, 2.64 Å, is close to these experimental findings. The estimated C_5—Cl distances, 3.164−3.163 Å, for **Ia** and **Ib**, also are close to the observed values,[33] 3.320-(9) and 3.239(11). Moreover, the calculated C_5−H_{13}—Cl angles, 109.4° and 109.3°, for **Ia** and **Ib**, are nearer to the observed range,[33] 117−118 °. Thus, these theoretical and experimental results suggest the formation of intramolecular C_5H_{13}—Cl H-bonds in **Ia** and **Ib.**

For the calculated planar structures of the **Ic** and **Id** derivatives, the C_5H_{13}—O_{14} contacts, 2.24 Å, are also noticeably smaller than the sum of the van der Waals radii of the oxygen (1.5 Å) and H atoms (1.1 Å), suggesting the appearance of C_5H_{13}—O_{14} hydrogen bonds in these molecules. Analyzing a database of X-ray structures, Taylor and Kennard[31] observed that the CH—O interaction is contained in the 2.04−2.39 Å range. From the theoretical point of view, using the B3LYP/6-31G(d,p) method, a value of 2.253 Å was found for the conventional intramolecular O—H bond of hydroxylthiophenol.[34] The present B3LYP/6-311++G-(d,p) results are in favor of the C_5H_{13}—O_{14} intramolecular hydrogen bond formation in each **Ic** and **Id** derivative; this, in addition to the $C_{11}H_{12}$—N_3 bonding, quoted above. Even

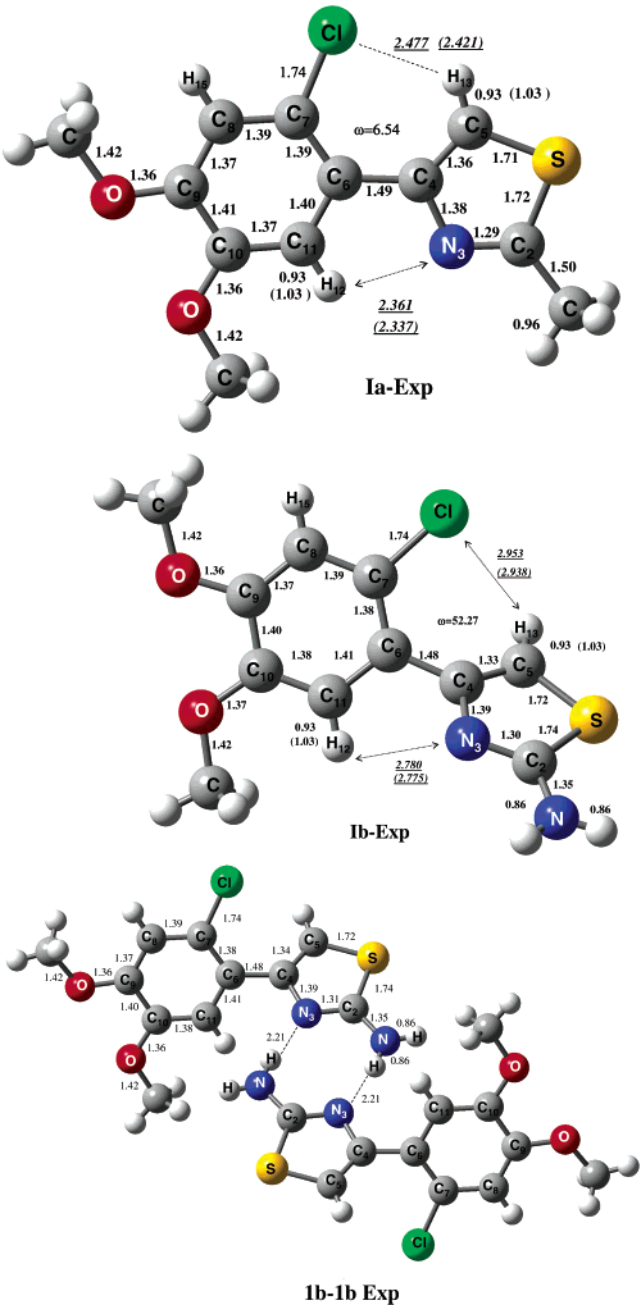

Figure 2. Experimental geometries for the **Ia (Ia-Exp)** and **Ib (Ib-Exp)** molecules and for the **Ib-Ib (1b-1b-Exp)** dimer. For **Ia** and **Ib** are indicated the neutron diffraction corrections for the C−H bond lengths and for the Cl−H distances.

more, our estimated C_5—O_{14} distances, 2.791 Å for **Ic** and 2.795 Å for **Id**, are shorter than the recommended value, 3.25 Å, for this type of CH—O bonding.[5]

Another property that allows depicting H-bonds is the C−H—X bond angle. Desiraju and Steiner[7] have found that very strong H-bonds have C−H—X angles of 175−180°, strong H-bonds may have 130−180°, but angles smaller than 130° imply the formation of weak H-bonds. The C_5—H_{13}—Cl bond angles for **Ia** and **Ib** are ≅109°, while smaller C_{11}—H_{12}—N_3 angles, of 101°, were computed for these species. Then **Ia** and **Ib** have weak CH—Cl bonds and, presumably, much weaker CH—N bonds.

Ic and **Id** follow the same trend, and they have C_5—H_{13}—O_{14} angles of ≅109° and C_{11}—H_{12}—N_3 angles of ≅103°. Why then in **Ic** and **Id** $C_{11}H_{12}$—N_3 and C_5—H_{13}—O_{14} bonds are formed, while in **Ia** and **Ib** only C_5H_{13}—Cl bonds are formed? The answer may be due to the fact that, as indicated by the $C_7C_6C_4C_5$ dihedral angle, **Ic** and **Id** are planar species, while this angle indicates a considerable deviation from planarity for **Ia** and **Ib**.

A property that determines the strength of the H-bond formation is the stabilization energy due to this kind of bond. For the intermolecular case, this property is estimated as the energy difference of two states of the AH and B units: the sum of the total energies of two independent AH and B ground states minus the total energy of the AH—B system, i.e., when the moieties are joined by H-bonds. However, in the intramolecular CH—X systems, both donor (CH) and acceptor (N, O, and Cl) fragments are contained within the **Ia**−**Id** thiazole derivatives, as they cannot be independent moieties. This feature requires the location of a structure where the intramolecular H-bond is absent or diminished. In an attempt to locate such "absent H-bond" structures, we have carried out total energy calculations for each **Ia**−**Id** derivative, varying the dihedral $C_5C_4C_6C_7$ angles. This rotation is allowed, since, although there is some small degree of π-conjugation between C_4 and C_6, the C_4−C_6 distance, 1.478 Å, indicates, essentially, a single C−C bond. The PESs for this rotational degree of freedom are shown in Figure 3. It should be pointed that at each selected dihedral angle (it was varied at intervals of 30°), a fully optimization, structural and electronic, was performed. The PESs are symmetrical around 180°. In the first step, the whole PES profile was obtained with the 6-31G(d,p) basis set. Afterward, with the purpose to obtain more accurate results, the important points (GS, 90, 120, and 180° points) were computed with the 6-311++G(d,p) basis; the values obtained are also indicated there.

The four **Ia**−**Id** curves present a similar pattern. The first local maximums, at 90°, are mainly due to the breaking of the small π conjugation between the phenyl and thiazole rings. In addition, these structures have slightly longer C_4−C_6 distances, ≅1.49 Å, than the ground-state geometries. (The C_4−C_6 distance is 1.48 Å for the ground states of **1a** and **1b**, and it is 1.47 Å for **1c** and **1d**, see Figure 1). Absolute maximums at 180° are mainly accounted by the manifestation of heteroatom repulsions, involving relatively high electronegative atoms: N_3—Cl for **Ia** and **Ib** and N_3—O_{14} for **Ic** and **Id**. Additionally, the H_{12}—H_{13} repulsions, in the four cases, also contribute to the energy increase. On the other hand, the minimums at 120° reflect the absence of such heteroatom and H_{12}—H_{13} repulsions as well as the absence of intramolecular H-bond formation, since the N_3—Cl, N_3—O_{14}, and H_{12}—H_{13} and the H—N, Cl—H, and O—H distances are quite big; see Figure 3. We have estimated the stabilization energy, due to intramolecular H-bonding, subtracting the total energy of the corresponding **Ia**−**Id** GS from the respective value at 120°. For the nonplanar GSs of **Ia** and **Ib** were obtained 2.1 kcal/mol for this property, at the B3LYP/6311++G(d,p) level of theory. While for **Ic** and **Id**, the stabilization energy is ≅4.1 kcal/mol. The quasiplanar geometry of **Ic** and **Id** coupled with the presence of the more electronegative O atoms is mainly responsible for the H-bond

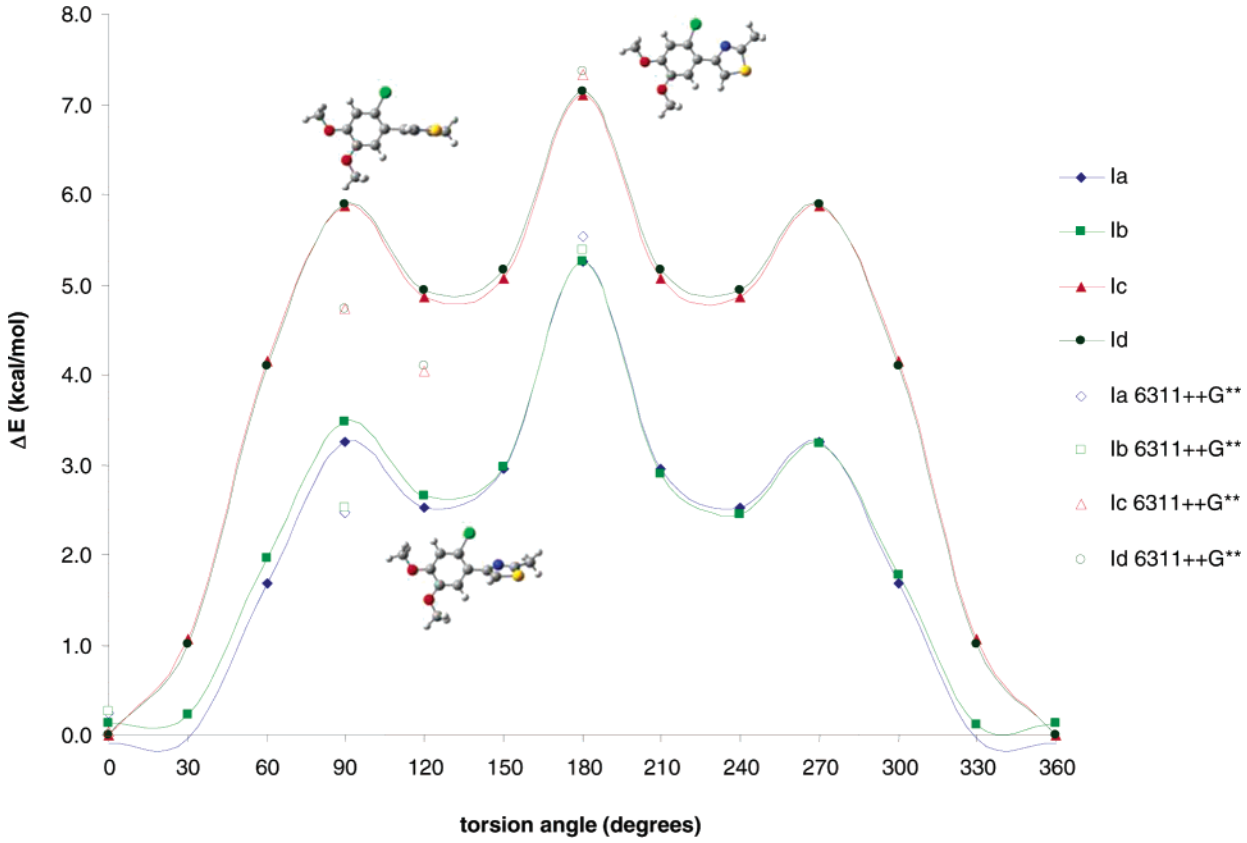

Figure 3. Potential B3LYP/6-31G(d,p) energy surfaces for **Ia**−**Id.** They were obtained through the variation, by steps of 30°, of the $\omega = C_7C_6C_4C_5$ dihedral angle. Also are indicated the B3LYP/6-311++G(d,p) results for the optimized **Ia**−**Id** structures at 90°, 120°, and 180°. In detail are shown the drawings for the corresponding structures at 0°, 90°, 120°, and 180° of the **Ia** molecule.

energy in these species. Then, this energetic criterion suggests the formation of weak intramolecular H-bonds in **Ia** and **Ib**. Below we will show, through the topological behavior of the electronic density, that in **Ia** and **Ib** only are formed intramolecular C_5H_{13}—Cl bonds; while two intramolecular H-bonds, CH—N and CH—O, are formed in each **Ic** and **Id** derivative. Indeed, the calculated H-bond energies account for the formation of two weak H-bonds in **Ic** and **Id**. Each $C_{11}H_{12}$—N_3 and C_5H_{13}—O_{14} contact will have, roughly, a H-bond energy of about 2.0 kcal/mol; this value falls within the assigned range, 2−5 kcal/mol, for weak H-bonds.[7] Moreover, the estimated H-bond energies of **Ia** and **Ib**, 2.0 kcal/mol, suggest the formation of a weak C_5H_{13}—Cl bond. According to Scheiner et al.,[35] the magnitude of this attractive weak interaction falls on the borderline, 2−3 kcal/mol, of true H-bonds.

It is important to highlight that the experimental geometry of **Ia** is quasiplanar, since the dihedral $C_7-C_6-C_4-C_5$ angle is 6.54°, while the X-ray structure of **Ib** is nonplanar with a dihedral $C_7-C_6-C_4-C_5$ angle of 52.24°. **Ia** has a methyl group in the C_2 position, and **Ib** has an amine group. This amine group may allow the formation of two intermolecular NH—N_3 bonds between two **Ib** molecules; see the structure **Ib-Ib-Exp** in Figure 2. These intermolecular NH—N_3 bonds account for the type of crystal structure showed by the **Ib** thiazole derivative, where **Ib** is rotated 52.27°. The intermolecular NH—N_3 bonding is the main trigger for the stabilization of such 52° **Ib** conformer or, so-called, rotamer. The B3LYP/6-311++G(d,p) binding energy of the two intermolecular N_3H—H bonds for the **Ib-Ib** dimer is equal to 8.2 kcal/mol, yielding 4.1 kcal/mol for each intermolecular N_3H—N bond; which is bigger than the stabilization energy, 2.1 kcal/mol, due to the intramolecular C_5H_{13}—Cl binding, obtained for the (gas phase) GS of **Ib**, where the dihedral angle is equal to 25.3°.

IIIb. Atoms in Molecules and Chemical Shifts Results. We will now address the analysis of the electronic densities, ρ, and Laplacians, $\nabla^2\rho$, of the intramolecular $C_{11}H_{12}$—N_3, C_5H_{13}—Cl, and C_5H_{13}—O contacts. For each **Ia**−**Id** ground-state structure was computed, using the code Gaussian-98, the corresponding B3LYP/6-311++G(d,p) wave function. Furthermore, these GS wave functions were used to determine BCPs and RCPs with AIM2000.[26,36] The obtained topological parameters are reported in Table 1 and in Figure 4 for **Ib**. For **Ia** and **Ib**, the AIM treatment defines clearly BCPs ($\rho = 0.0125$ e au^{-3} and $\nabla^2\rho = +0.0468$ e au^{-5}) along the C_5H_{13}—Cl paths; see Figure 4. Note that the values for the Laplacians are positive, as expected for a weak H-bond. Consistently, the six member rings, originated by the H_{13}—Cl bonds, show quite defined RCPs ($\rho = 0.0093$ e au^{-3} and $\nabla^2\rho = +0.0452$ e au^{-5}); although, due to the asymmetry, they are somehow deviated from the center. For instance, in the phenyl and thiazole groups, the RCPs are located at the center of the rings. See Figure 4.

On the other hand, the C_5H_{13}—O_{14} and $C_{11}H_{12}$—N_3 paths of **Ic** and **Id** define clearly the appearance of BCPs and

Table 1. Calculated B3LYP/6-311++G(d,p) Density (ρ), in e au^{-3}, and Laplacians ($\nabla^2\rho$), in e au^{-5}, for the Bond Critical Points (BCP) and Ring Critical Points (RCP) of the CH—N, CH—Cl, and CH—O Contacts of the **Ia**−**Id** Ground States

		ρ_{BCP}	$\nabla^2\rho_{BCP}$	ρ_{RCP}	$\nabla^2\rho_{RCP}$
Ia	C−H−N				
	C−H−Cl	0.0125	0.0468	0.0093	0.0452
Ib	C−H−N				
	C−H−Cl	0.0125	0.0468	0.0093	0.0452
Ic	C−H−N	0.0158	0.0692	0.0158	0.0796
	C−H−O	0.0168	0.0684	0.0109	0.0636
Id	C−H−N	0.0157	0.0688	0.0157	0.0784
	C−H−O	0.0168	0.0684	0.0109	0.0632

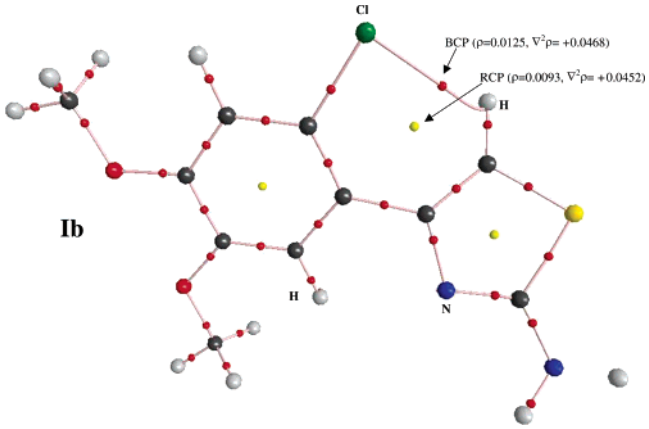

Figure 4. Molecular graph for the GS of **Ib**. The B3LYP/6-311++G** density (ρ), in e au^{-3}, and laplacians ($\nabla^2\rho$), in e au^{-5}, are indicated for the BCP of the CH—Cl contact and the RCP for the ring.

RCPs; see Table 1. In fact, of the studied species, these compounds show the shorter C_5H_{13}—O_{14} and $C_{11}H_{12}$—N_3 contacts, where the former is the shortest one. The AIM results for the C_5H_{13}—O_{14} BCPs (ρ = 0.0168 e au^{-3} and $\nabla^2\rho$ = +0.0684 e au^{-5}) and the values for the $C_{11}H_{12}$—N_3 BCPs (ρ = 0.0157−0.0158 e au^{-3} and $\nabla^2\rho$ = +0.0688 − +0.0692 e au^{-5}) of **Ic** and **Id**, see Table 1, are in agreement with the topological criteria for the existence of H-bonds as given by Koch and Popelier:[13] 0.002−0.035 e au^{-3} for the electronic density and 0.024−0.139 e au^{-5} for the associated Laplacian.

Aside from the AIM evidence of CH—X (X = Cl and O) bonding, it was found that the highest occupied molecular orbital (HOMO) of **Ia** and **Ib**, shown in Figure 5, has signatures of bonding interactions for C_5—H_{13}—Cl. Also the HOMOs of **Ic** and **Id** reveal bonding interactions for C_5—H_{13}—O.

The AIM results for the experimental geometry of **Ia** reveal the formation of a C_5—H_{13}—Cl intramolecular H-bond and the absence of C_{11}—H_{12}—N_3 bonding. This picture is similar to that found for **Ia** in the gas phase. **Ia** is quasiplanar, both in the gas phase and in the crystal; see Figures 1 and 2. However, for the experimental geometry of **Ib** AIM indicates the absence of C_5—H_{13}—Cl and C_{11}—H_{12}—N_3 intramolecular H-bonds, which may be due to a large deviation from planarity of **Ib** in the crystal. The deviation may be due to

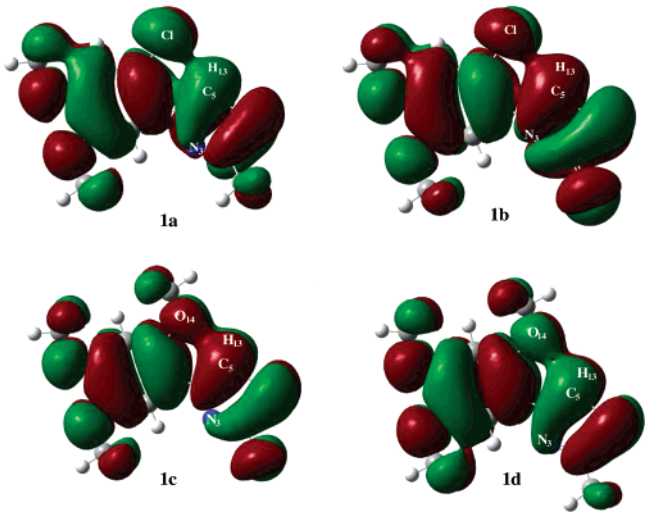

Figure 5. Contour plots of the higher occupied molecular orbitals (HOMO) for the GSs of **Ia**−**Id**. The HOMOs contain signatures of C−H−X, (X = Cl and O) bonding interactions.

the intermolecular H-bonding that may occur among the **Ib** units in the crystal. We have also performed AIM calculations for the **Ib-Ib** dimer, labeled as **Ib-Ib-Exp** in Figure 2, where the bond lengths and angles are equal to the experimental values. The results indicate the formation of two intermolecular NH—N_3 bonds between two **Ib** units; see Figure 6. As quoted, B3LYP/6-311++G(d,p) indicates a binding energy of 8.2 kcal/mol for **Ib-Ib**, yielding 4.1 kcal/mol for each N−H—N_3 bond; which is a bigger value than the binding energy of the C_5—H_{13}—Cl intramolecular H-bond calculated for **Ib** in the gas phase, about 2.1 kcal/mol.

Finally, a theoretical study of the chemical shifts in the ^{1}H NMR was made by the GIAO method at the B3LYP/6-311++G(d,p) electronic level of treatment. This approach also may be useful for a potential identification of H-bonds.[35,37−39] The calculated chemical shifts, in ppm, for some representative hydrogen atoms of the **Ia**−**Id** species are reported in Table 2; in parentheses are indicated the experimental values.[2] These theoretical results are in close agreement with the values obtained experimentally[2] by ^{1}H NMR. For example, the calculated chemical shifts of the H_{12} and H_{13} atoms are overestimated by 0.35−0.52 ppm, while underestimations of 0.22−0.40 ppm were obtained for H_{15}; see Table 2. For **Ia** and **Ib** there is no clear correlation between shifts and H-bond formation. For instance, in **Ia**, H_{12} and H_{13} have very similar values, 7.92 and 7.98 ppm, respectively, which are bigger, by 1.24−1.30 ppm, than the value for H_{15}. The experiment also indicates similar shifts for H_{12} and H_{13}, bigger than that of H_{15}. However, as shown above, H_{12} does not form an H-bond. Moreover, in **Ib**, the shift of H_{12} (not forming a H-bond) is bigger, by 1.25 ppm, than that of H_{15}; but H_{13} (forming a H-bond) has a smaller difference, 0.82 ppm, from the value of H_{15}. The experiment also yields a smaller difference between the shifts of H_{13} and H_{15}. That is, in **Ia** and **Ib**, there is not a clear correlation between chemical shifts and H-bonds. In these cases, the shifts are merely due to the different topological positions of the H atoms. A different behavior is observed for **Ic** and **Id**, since the H_{12} and H_{13} centers of these moieties, which

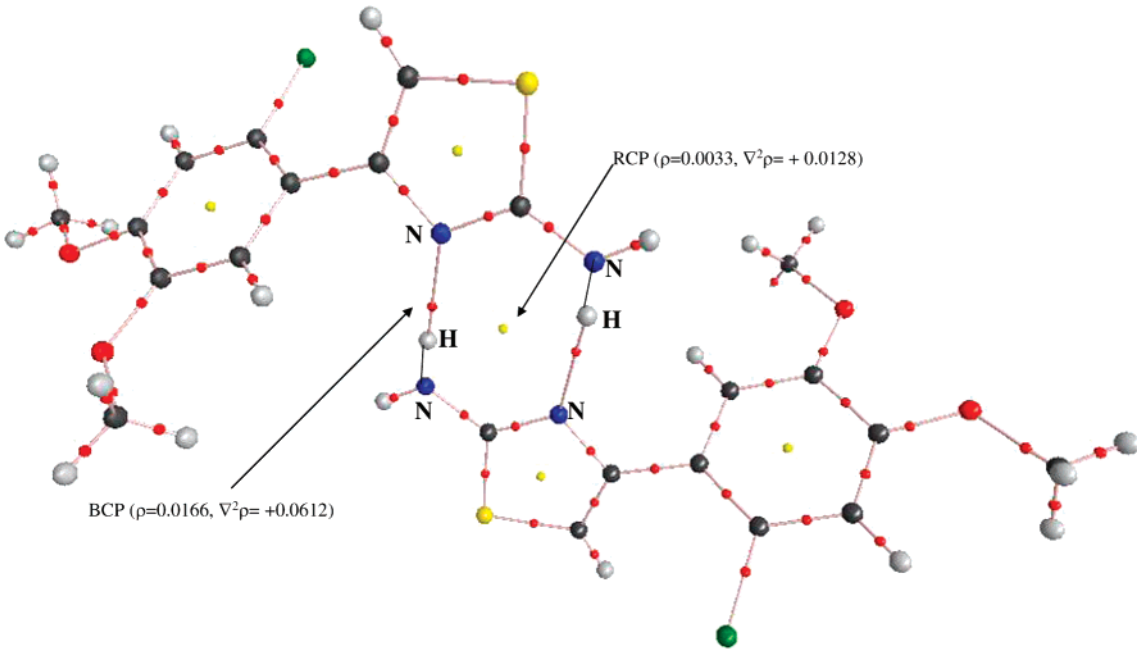

Ib-Ib-Exp

Figure 6. Molecular graph for the **Ib-Ib** dimer (**Ib-Ib-Exp**). The calculated B3LYP/6-311++G** density (ρ), in e au-3, and laplacianes ($\nabla 2\rho$), in e au-5, are indicated for the BCPs of the intermolecular N—H—N and N—H—N hydrogen bonds. Note the appearance of the associated RCP.

Table 2. Calculated GIAO B3LYP/6-311++G(d,p) Chemical Shifts, in ppm, for the Benzene H_{12} and Thiazole H_{13} Atoms, Involved in the H-Bond Interactions and for the Aromatic H_{15} Atoms not Forming H-Bonds[a]

	H_{12}	H_{13}	H_{15}
Ia	7.92	7.98	6.68
	(7.51)	(7.63)	(6.93)
Ib	7.94	7.51	6.69
	(7.42)	(7.04)	(6.91)
Ic	8.06	7.59	6.17
	(7.63)	(7.08)	(6.57)
Id	8.38	8.25	6.25
	(7.90)	(7.74)	(6.63)

[a] The experimental values are shown in parentheses.

form clearly H-bonds, have shifts that are significantly bigger, 1.42−1.89 ppm, than that of the H_{15} atom. In other words, in **Ic** and **Id** the chemical shifts of the H_{12} and H_{13} centers have signatures of H-bonds. The magnitude of these shifts is in agreement with the estimated higher H-bond energy, 4.1 kcal/mol for **Ic** and **Id**, and with the topological results from AIM, which show the formation of two, C_5H_{13}—O_{14} and $C_{11}H_{12}$—N_3, H-bonds.

Conclusions

The nonconventional CH—X (X = N, O, or Cl) H-bonds formed intramolecularly in the **Ia**−**Id** thiazoles were studied by means of calculations made with the B3LYP/6-311++G-(d,p) method. The obtained results for the geometrical, energetic, topological, and spectroscopic properties allowed the characterization of these H-bonds. The computed properties for the bare GSs suggest the formation of one H-bond, CH—Cl, in **Ia** and **Ib**; in these species the CH—N bond is absent, while two H-bonds, CH—N and CH—O, are formed in **Ic** and **Id.** Indeed, the geometrical criteria indicate that the H—Cl distances, 2.64 Å, of **Ia** and **Ib** and the H—N and H—O lengths, 2.34−2.35 and 2.24 Å, respectively, of **Ic** and **Id** are noticeably shorter than the respective sum of the X and H van der Waals radii. Consistently, according to the theory of atoms in molecules, the electronic density shows bond critical points for the CH—X bonds. The weak character of these H-bonds is indicated by the H-bond energies, which are ≅2.1 kcal/mol for **Ia** and **Ib** and ≅4.1 kcal/mol for **Ic** and **Id**. Deviation from planarity also is important; **Ia** and **Ib** with nonplanar structures have only one H-bond, CH—Cl, whereas **Ic** and **Id** with quasi-planar geometries have two H-bonds, CH—O and CH—N. Moreover, in the crystal **Ib** is largely deviated from planarity, avoiding the formation of intramolecular CH—X bonds; instead, there are formed two intermolecular NH—N bonds between two **Ib** units. This N—H—N bond is stronger than the C—H—Cl bond of **Ib** in the gas phase. The chemical shifts in the ^{1}H NMR were also calculated by the GIAO method. In **Ia** and **Ib** they are merely due to the different topological positions of the H atoms. But in **Ic** and **Id** the shifts in H—N and H—O have signatures of H-bond formations.

Acknowledgment. We acknowledge financial support from DGAPA-UNAM under Project PAPIIT: IN-107905. J. I. Zavala appreciates a scholarship from these sources. I. Nicolás-Vázquez deeply thanks CONACyT-México and DGAPA-UNAM (PASPA) for a grant. The access to the supercomputer facilities at DGSCA-UNAM is strongly

appreciated. Dr. Alfredo Vazquez is thanked for valuable discussions. The referee's suggestions are deeply acknowledged.

Supporting Information Available: Selected equilibrium bond lengths and bond and dihedral angles (Tables 1−3). This material is available free of charge via the Internet at http://pubs.acs.org.

References

(1) Joule, J. A.; Mills, K. 1,3-Azoles: imidazoles, thiazoles, and oxazoles: reactions and synthesis. In *Heterocycle chemistry*, 4th ed.; Blackwell Sciences Publishing: Oxford, U.K., 2002; pp 402−425.

(2) Sánchez-Viesca, F.; Berros, M. *Heterocycles* **2002**, *57*, 1869−1879.

(3) Bernés, S.; Berros, M. I.; Rodríguez de Barbarín, C.; Sánchez-Viesca, F. *Acta Crystallogr., Sect. C: Cryst. Struct. Commun.* **2002**, *C58*, o151−o153.

(4) Castellano, R. K.; Diederich, E. A.; Meyer, E. A. *Angew. Chem., Int. Ed. Engl.* **2003**, *42*, 1210−1250.

(5) Desiraju, G. R. *Acc. Chem. Res*. **2002**, *35*, 565−573.

(6) Dinçer, M.; Özdemir, N.; Çukurovali, A.; Yilmaz, I. *Acta Crystallogr., Sect. C: Cryst. Struct. Commun.* **2005**, *E61*, o1712−o1714.

(7) Desiraju, G. R.; Steiner The Hydrogen Bond. In *The weak hydrogen bond in structural chemistry and biology*, 1st ed.; Oxford University Press, Inc.: New York, 1999; pp 1−28.

(8) Grabowski, S. J. *J. Phys. Org. Chem*. **2004**, *17*, 18−31.

(9) Grabowski, S. J.; Pfitzner, A.; Zabel, M.; Dubis, A. T.; Palusiak, M. *J. Phys. Chem. B* **2004**, *108*, 1831−1837.

(10) Domagala, M.; Grabowski, S. J.; Urbaniak, K.; Mlostoń, G. *J. Phys. Chem. A* **2003**, *107*, 2730−2736.

(11) Dubis, A. T.; Grabowski, S. J.; Romanowska, D. B.; Misiaszek, T.; Leszczynski, J. *J. Phys. Chem. A* **2002**, *106*, 10613−10621.

(12) Bader, R. F. W. Atoms and the topology of the charge density, Chemical bonds and molecular graphs. In *Atoms in Molecules. A Quantum Theory*, 1st ed.; Oxford University Press: New York, 1990; pp 32−35.

(13) Koch, U.; Popelier, P. L. A. *J. Phys. Chem*. **1995**, *99*, 9747−9754.

(14) Bickelhaupt, F. M.; Baerends, E. J. Kohn-Sham Density Functional Theory: Predicting and understanding chemistry. In *Reviews in Computational Chemistry*, 1st ed.; Lipkowitz, K. B., Boyd, D. B., Eds.; Wiley-VCH, John Wiley and Sons, Inc.: New York, 2000; Vol. 15, pp 1−86.

(15) Becke, A. D. *J. Chem. Phys*. **1993**, *98*, 5648−5652.

(16) Lee, C.; Yang, W.; Parr, R. G. *Phys. Rev*. **1988**, *B37*, 785−789.

(17) Calhorda, M. J. *Chem. Commun*. **2000**, 801−809.

(18) Richardson, T. R.; Gala, S.; Crabtree, R. H.; Siegbahn, P. E. M. *J. Am. Chem. Soc*. **1995**, *117*, 12875−12876.

(19) Orlova, G.; Scheiner, S. *J. Phys. Chem. A* **1998**, *102*, 260−269.

(20) Orlova, G.; Scheiner, S. *J. Phys. Chem. A* **1998**, *102*, 4813−4818.

(21) Adotöledo, D.; Aviyenta, V.; Martin, J. M. L.; Lifshitz, C. *J. Phys. Chem. A* **1998**, *102*, 6357−6365.

(22) Rablen, P. R.; Lockman, J. W.; Jorgensen, W. L. *J. Phys. Chem. A* **1998**, *102*, 3782−3797.

(23) Chung, G.; Kwon, O.; Kwon, Y. *J. Phys. Chem. A* **1998**, *102*. 2381−2387.

(24) . Alkorta, I.; Rozas, I.; Elguero, J. *Theor. Chem. Acc*. **1998**, *99*, 116−123.

(25) Frisch, M. J.; Trucks, G. W.; Schlegel, H. B.; Gill, P. M. W.; Johnson, B. G.; Robb, M. A.; Cheeseman, J. R.; Keith, T. A.; Petersson, G. A.; Montgomery, J. A.; Raghavachari, K.; Al-Laham, M. A.; Zakrzewski, V. G.; Ortiz, J. V.; Foresman, J. B.; Cioslowski, J.; Stefanov, B.; Nanayakkara, A.; Challacombe, M.; Peng, C. Y.; Ayala, P. Y.; Chen, W.; Wong, M. W.; Andres, J. L.; Replogle, E. S.; Gomperts, R.; Martin, R. L.; Fox, D. J.; Binkley, J. S.; Defrees, D. J.; Baker, J.; Stewart, J. J. P.; Head-Gordon, M.; Gonzalez, C.; Pople, J. A. *GAUSSIAN 98 (Revision C.3)*; Gaussian Inc.: Pittsburgh, PA, 1998.

(26) AIM2000 designed by Friedrich Biegler-König, University of Applied Sciences, Bielefeld, Germany, 2000.

(27) Popelier, P. Bond characterization. In *Atoms in Molecules. An Introduction*, 1st ed.; Prentice Hall, Pearson Education Limited: Englewood Cliffs, NJ, 2000; pp 150−156, 113.

(28) Ditchfield, R. *Mol. Phys*. **1974**, *27*, 789−807.

(29) Wolinski, K.; Hinton, J. F.; Pulay, P. *J. Am. Chem. Soc*. **1990**, *112*, 8251−8260.

(30) Cotton, F. A.; Daniels, L. M.; Jordan IV, G. T.; Murillo, C. A. *Chem. Commun*. **1997**, 1673−1674.

(31) Bondi, A. J. *Phys. Chem*. **1964**, *68*, 441−451.

(32) Taylor, R.; Kennard, O. *J. Am. Chem. Soc*. **1982**, *104*, 5063−5070.

(33) Moro, A. C.; Watanabe, F. W.; Ananias, S. R.; Mauro, A. E.; Netto, A. V. G.; Lima, A. P. R.; Ferreira, J. G.; Santos, R. H. A. *Inorg. Chem. Commun.* **2006**, *9*, 493−496.

(34) Chung, G.; Kwon, O.; Kwon, Y. *J. Phys. Chem. A* **1997**, *101*, 9415−9420.

(35) Scheiner, S; Gu, Y.; Kar, T. *J. Mol. Struct.* (THEOCHEM) **2000**, *500*, 441−452.

(36) Rozas, I.; Alkorta, I.; Elguero, J. *J. Phys. Chem. A* **2001**, *105*, 10462−10467.

(37) Scheiner, S.; Grabowski, S. J.; Kar, T. *J. Phys. Chem. A* **2001**, *105*, 10607−10612.

(38) Mizuno, K.; Ochi, T.; Shindo, Y. *J. Chem. Phys*. **1998**, *109*, 9502−9507.

(39) Alkorta, I.; Elguero, J. *New J. Chem*. **1998**, 381−385.

CT600336R